JOURNAL OF APPLIED ELECTROCHEMISTRY **29**: 239–244, 1999.

Corrosion of cyanide copper deposits on zinc diecastings in acid solutions

T. F. OTERO

Laboratorio de Electroquímica, Facultad de Químicas, Apdo 1072, San Sebastián, Spain

J. L. RODRÍGUEZ-JIMÉNEZ

Departamento de Investigación y Desarrollo, Egoki S. Coop. Ltda, Irún, Spain

Received 17 November 1997; accepted in revised form 30 June 1998

The corrosion potential and morphology of copper films deposited from a cyanide solution on zinc diecast were studied in acid solutions similar to those employed in industry for the deposition of a second copper layer. Open circuit potential measurements and gravimetric methods were employed to determine the influence of the copper electrodeposition variables on the corrosion potential. The influence of variables such as the presence or absence of additives, the current density and the copper or cyanide concentrations were studied. The corrosion potential decreased with increasing copper film thickness. Less protection was obtained when a thin copper layer was electrodeposited from a solution without additives. Higher protection for the same thickness was obtained from a solution with high cyanide content. This result is related to the strong interaction between cyanides and the metal surface during the electrodeposition. A smooth surface structure was observed by SEM under these conditions.

Keywords: *acid solution*, *copper*, *corrosion potential*, *cyanide*, *electrodeposition*, *zinc diecast*

List of symbols

A	preexponential factor (V)
A_a	anodic area, Zn (cm^2)
A_c	cathodic area, Cu (cm^2)
b_a	anodic Tafel slope (V)
b_c	cathodic Tafel slope (V)
δ	thickness of copper film (μm)
η_a	anodic overpotential (V)
η_c	cathodic overpotential (V)
η	mixed corrosion potential (V)
η_0	steady state potential at high thickness (V)
I_a	anodic current (A)
i_a	anodic current density ($A\,cm^{-2}$)
I_c	cathodic current (A)
i_c	cathodic current density ($A\,cm^{-2}$)
i_{0a}	anodic exchange current density ($A\,cm^{-2}$)
i_{0c}	cathodic exchange current density ($A\,cm^{-2}$)

1. Introduction

A metal can be covered with metallic coatings for many different reasons. These can include enhancing the solderability or contact properties, improving the wear resistance or decorative purposes. The most common and important function of such coatings, however, is to resist the corrosive action of the environment. If a metal coating can be deposited without impurities and without discontinuities, its behaviour is essentially that shown by the metal itself. Unfortunately, this is difficult to achieve since discontinuities in a coating can have a considerable effect on its corrosion behaviour: their study is important in order to determine protection properties.

The porosity of a coating is related to its corrosion resistance. Generally, therefore, the porosity of a coating is important when the coating acts as cathode in a bimetallic corrosion cell but unimportant if it acts as the anode [1]. In the case of decorative electroplating improved durability of bright coatings has been achieved by electrodeposition of a three-metal multilayer of copper–nickel–chromium [2]. The improvement has extended the corrosion protection and good appearance of plated commodity materials, like zinc diecast or zamak, containing zinc with 4% of aluminium and 1% of copper. From the viewpoint of the corrosion behaviour zinc diecast behaves like zinc.

Zinc diecast specimens are often plated with copper, nickel and chromium for protection and decoration. When zinc is immersed in a typical copper acid plating solution, which provides a brilliant surface, it corrodes rapidly and dissolves in the acid bath. If a specimen is immersed with current flow, corrosion and electrodeposition occur simultaneously. In standard practice the zinc is first plated with an undercoat from a cyanide copper bath. This deposited film is too noble to dissolve in the acid solution [3].

Stabilities of zinc and copper are reversed in alkaline cyanide, and zinc will not displace copper from cuprocyanide solutions [4]. Once a coherent copper coating envelopes the zinc, the specimen is transferred to the copper acid bath. However, plates are porous [5] and the specimens have a complex shape giving a nonuniform coating. Thus, diecasting zones do not have full coverage and the acid bath will attack the substrate resulting in severe corrosion. Under these conditions it is important to know the porosity in order to improve the electroplating conditions attaining a most compact electrodeposit.

Previous studies focused on the influence of the plating bath components on the porosity [6–14]. Notter and Gabe say that alkaline cyanides bath are often thought to give lower coating porosity because these plating solutions are suitable for cleaning the substrate during plating [5]. The addition of brightening agents to a plating bath has been shown, in most circumstances, to reduce the porosity of an electrodeposit [9]. Leeds [11] has attributed that reduction to the tendency of brighteners to promote lateral crystal growth in a deposit, thus enhancing the rate of pore sealing.

Current density may significantly affect the porosity: low current densities during electrodeposition give a more compact deposits [12–14, 8]. Similar results have also been obtained by Leeds [7]. At increasing agitation rates, he noticed that the porosity drops to a minimum and then rises again.

In this paper porosity will be indirectly evaluated by corrosion potential measurements. When two metals are coupled in an appropriate electrolyte, the corrosion potential is a function of the relative surface area of each metal. Therefore, any variation on the porosity (and hence on the area of the exposed substrate) will result in a shift of the corrosion potential. The first systematic investigation based on experimental determination of the corrosion potential in order to test the porosity was performed by Morrissey [15] who studied gold coatings on copper. Morrissey established that the corrosion potential of a specimen was related to the logarithm of the fraction of exposed area. This relationship was valid for thin coatings. Oldham and Mansfeld [16] attributed the deviation from this behaviour at high thickness to a third reaction, such as the H_2 or OH^- oxidation on the coating.

In acid solution, when a metal corrodes, the anodic current of the metal dissolution and the cathodic current of the hydrogen evolution must be the same. The corrosion potential was calculated from the Tafel equations when both anodic and cathodic currents equalize [17]. Thus, if we consider the reactions:
Anodic (a) on Zn:

$$Zn - 2e^- = Zn^{2+} \tag{1}$$

Cathodic (c) on Cu:

$$2H_3O^+ + 2e^- = H_2 + 2H_2O \tag{2}$$

under steady state:

$$I_a = I_c \tag{3}$$

$$i_a A_a = i_c A_c \tag{4}$$

$$i_a / i_c = A_c / A_a \tag{5}$$

This process is controlled by activation polarization [17] and it is possible to use the following equations:

$$i_a = i_{0a} \exp(\eta_a / b_a) \tag{6}$$

$$i_c = i_{0c} \exp(-\eta_c / b_c) \tag{7}$$

Combination of Equations 5, 6 and 7 gives:

$$\frac{i_a}{i_c} = \frac{A_c}{A_a} = \frac{i_{0a}}{i_{0c}} \exp\left[\eta\left(\frac{1}{b_a} + \frac{1}{b_c}\right)\right] \tag{8}$$

Taking logarithms yields:

$$\eta = C\left[\frac{2.3\, b_a b_c}{(b_a + b_c)} \log\left(\frac{A_c}{A_a}\right)\right] \tag{9}$$

where

$$C = -\frac{b_a b_c}{(b_a + b_c)} \ln\left(\frac{i_{0a}}{i_{0c}}\right) \tag{10}$$

Equation 9 is a general expression for any galvanic couple, such as Cu/Zn. The slope of this curve contains b_a and b_c, the anodic Tafel slope of the substrate and the cathodic Tafel slope of the coating material, respectively.

Most work related to the use of copper cyanide bath was performed in an attempt to replace cyanide by pyrophosphate [18], glycerol [19] etc., but adhesion problems hindered any practical application of these baths. Other groups used different brighteners in cyanide baths [20–22]. Few efforts were devoted to the study of the protection of zinc diecast in acid solution, in spite of the widespread industrial use of these baths.

The aim of this work was to investigate how the electrodeposition conditions of the copper films, generated from cyanide baths, influence the protection of zinc diecast when the electrodeposited samples were transferred into the acid copper bath. The corrosion potentials of the coated specimens were measured in the acid solution, and the porosity of each sample was estimated. The morphology of the coated specimens was observed by SEM.

2. Experimental details

The composition of the standard cyanide bath was: 70.5 g dm^{-3} CuCN (50 g dm^{-3} copper), 132.2 g dm^{-3} KCN (30 g dm^{-3} cyanide), 40 g dm^{-3} grain refining agent 5 ml dm^{-3} commercial surfactant cupralite 150 (Enthone–OMI) and 5 ml dm^{-3} commercial brightener cupralite 150 (Enthone–OMI). Deionized water (Milli RO4 water purification system) was used to prepare the solutions. The pH of the working solutions was 12. Technical reagents were used and the composition of the solution was similar to that of industrial baths. The standard conditions were: room temperature, a current density of 0.015 A cm^{-2} and a deposition time of 15 min.

Electrochemical experiments were performed in a single-compartment cell. Zinc diecast working electrodes having a surface area of 10.8 cm^2 were used. As counter electrode, a copper sheet of 20 cm^2 of surface area was used. A Ag/AgCl electrode was employed as reference electrode. All potentials are referred to this electrode.

The composition of the zinc diecast was: 95% zinc, 4% aluminium and the remainder copper. The cleaning treatment of the working electrodes followed the sequence:

(i) Cathodic electrocleaning at −4 V for 120 s in a commercial solution (Enprep 221).
(ii) Anodic electrocleaning at 4 V for 10 s in a commercial solution (Enprep 221).
(iii) Rinsing in deionized water.
(iv) Acid dipping in 1% H_2SO_4 until hydrogen bubbling.
(v) Rinsing in deionized water.

The zinc concentration in a fresh industrial acid copper bath was followed by atomic absorption using a Perkin Elmer 2380 espectrophotometer. The corrosion test was performed in a solution containing 60 g dm^{-3} H_2SO_4 and 0.17 g dm^{-3} NaCl, similar to an industrial acid copper bath. A 501 B Philips SEM microscope was used to observe the surface morphology.

The thickness of each copper film was obtained by gravimetric determination of the copper deposited on the electrode, using a Sartorius ultramicrobalance 4504 MPS (10^{-7} mg precision). Taking into account that the area of the electrode was 10.8 cm^2 and that the copper density is 8.92 g cm^{-3} [23], the average thickness of each film was calculated.

3. Results and discussion

3.1. *Preliminary study*

Factory plated zinc specimens from a cyanide bath were transferred into the acid bath where the copper electroplating was completed. The copper film deposited from alkaline copper baths is known to be nonuniform, because zinc corrosion occurs through the copper pores after immersion in the acid bath. Even when current flow starts the chemical corrosion process continues in parallel with the electrodeposition. The result is a continuous increase in the bath zinc content with time (Fig. 1). The copper acid bath becomes useless when the Zn concentration reaches a value between 8 and 10 g dm^{-3}. Under these conditions, the zinc present in the acid bath alters the passive film of CuCl coating the Cu anodes by modifying the electrode surface during the open circuit time. When the current flows again, small particles are detached from the anode promoting the formation of nodules on the zinc diecast specimens, giving a gritty appearance to the surface. The presence of a high Cl^- concentration in the bath initially eliminates these problems. However, in the long term nodule formation reappears, which, together with other additional problems linked to a high Cl^- concentration, makes this alternative unsuitable.

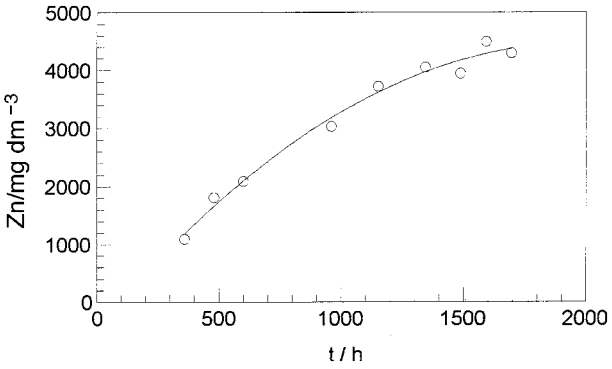

Fig. 1. Variation of zinc content in an industrial copper acid bath 200 g dm^{-3} $CuSO_4$, 60 g dm^{-3} H_2SO_4, 0.17 g dm^{-3} NaCl and additives as a function of the electrodeposition time. A surface of $2 \times 10^5/cm^2$ was treated per hour.

The nonuniformity of the deposits obtained from alkaline copper baths can be attributed to the presence of pores, allowing access of the acid solution to the base metal. When a specimen has pores or a partial coating its electrochemical potential in acid solution is midway between those of copper and zinc.

Equation 9 was checked using copper samples coupled to zinc diecast. The overall area of the two materials was kept constant and equal to 10.8 cm^2. The relative area (A_c/A_a) was changed for every experiment. A macroscopic calibration was obtained by measuring the steady state potential of a coupled sample (Fig. 2). This calibration curve shows that the corrosion potential increases when $\log(A_c/A_a)$ increases. Our experimental linear relationship is similar to the theoretical conclusion of Morrissey obtained for copper coated by gold [15]. A potential of −0.79 V vs Ag/AgCl was obtained when both metals have the same area. The corrosion potential shifts from −0.66 to −0.874 when the A_c/A_a fraction

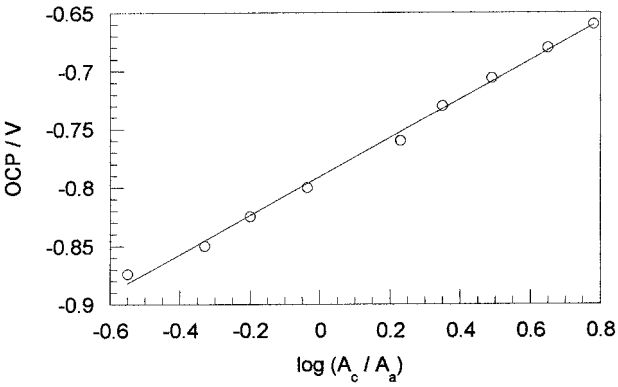

Fig. 2. Semilogarithmic plot of corrosion potential against the fraction of the cathodic and anodic areas. Measurements performed in a solution containing 60 g dm^{-3} H_2SO_4 and 0.17 g dm^{-3} NaCl for 30 min at room temperature. Working electrodes: 0.108 dm^2 of total surface area. Area fractions of copper 0.28, 0.47, 0.63, 0.92, 1.7, 2.24 and 3.1.

(A_{Cu}/A_{Zn}) goes from 6 to 0.31. The experimental corrosion potential value obtained using pure zinc diecast in the solution test was −0.9 V, while that of pure copper was 0.0 V. The A_c/A_a fraction is proportional to the porosity or number of pores per cm^2 present in the sample coated by copper.

3.2. *Corrosion potential experiments using zinc diecast specimens coated by copper from cyanide baths*

Specimens coated by copper having different thicknesses were obtained by changing one of the electrodeposition variables each time: electrodeposition time (with and without additives), current density, copper concentration and cyanide concentration. Figure 3 shows the open circuit potentials from samples coated at different electrodeposition times. A steady state potential is obtained after immersion for 20 to 30 min in the solution test. The range of the obtained experimental potentials overlaps the calibration curve (Fig. 2). Thus, the A_c/A_a fractions can be obtained for each specimen. The values obtained range from 5.4 to 0.5 when the thickness of the copper film changes between 7.7 and 0.6 μm.

Figure 4 shows the steady state corrosion potentials obtained after immersion for 30 min as a function of the copper film thickness. The potential drops exponentially when the copper thickness increases following the expression:

$$\eta = \eta_0 + A\exp(-\delta/\tau) \tag{11}$$

Taking logarithms,

$$\ln(\eta - \eta_0) = \ln A - \delta/\tau \tag{12}$$

The parameter $1/\tau$, obtained from the slope of a $\ln(\eta - \eta_0)$ against δ plot, is indicative of the efficiency of the thickening process in order to eliminate the porosity. The porosity depends on the grain size, which is determined by the synthesis conditions. Figure 4 also shows that at high thicknesses ($d > 4\,\mu$m), a given thickness increment provides a lower change in the corrosion potential and, consequently, a low change in the porosity. Thus, under these experimental conditions, it is difficult to achieve A_c/A_a fractions greater than 5.5, that is, more than 85% of the specimen area.

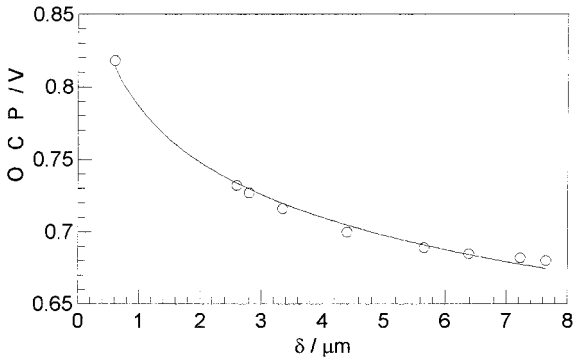

Fig. 4. Plots of OCP or corrosion potential against thickness of copper deposit constructed on the basis of curves shown in Fig. 2.

Experimental results similar to those presented in Fig. 4 were obtained by changing other experimental variables. Experiments were performed in the presence and absence of additives; current density was varied between 0.005 and 0.03 A cm^{-2}, copper concentrations were investigated in a 20 to 100 g dm^{-3} range, and cyanide concentration varied from 0 to 100 g dm^{-3}. The $1/\tau$ values obtained from these experiments are presented in Table 1. Coatings obtained in the absence of additive gave the greatest porosity, while the increase in cyanide concentration in the bath provided the most compact copper films. Specimens coated with thin films obtained at low current density, or from a bath with low copper concentration, had lower porosity than those obtained from the standard bath.

High cyanide concentrations in the bath increase the polarisation through the formation of a cyanide barrier on the cathode [3]. However, the most important effect on the porosity may be due to the preparation of a cleaner surface by complexing and subsequent elimination of impurities, which favour compactness [5]. The change in copper concentration had a lower influence on the porosity than the cyanide concentration.

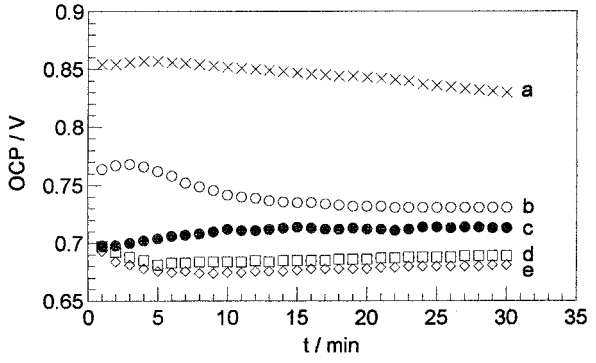

Fig. 3. Dependence of the open circuit potential (OCP) on immersion time in a solution with 60 g dm^{-3} H_2SO_4 and 0.17 g dm^{-3} NaCl. Curves correspond to thickness of copper deposit: (a) 0.6, (b) 2.6, (c) 3.3, (d) 5.7 and (e) 7.7 μm (Select curves are shown for clarity).

Table. 1. Dependence of slope ($1/\tau$) on the method for thickness variation

Synthesis conditions	*Without additives*	*Time* /min	*Current density* /A cm^{-2}	*Copper* /g dm^{-3}	*Cyanide* /g dm^{-3}
$\tau^{-1}/\mu m^{-1}$	−0.106	−0.47	−0.635	−0.708	−1.953

(No additives) without additives at different times of current flow: 2, 5, 7, 10, 12, 15, 17, 20 and 22 min
With additives, *t*: 2, 5, 10, 12, 15, 20 min
(*i*) at constant polarization time and constant composition changing the current density: 0.005, 0.01, 0.015, 0.02, 0.025, 0.03 A cm^{-2}
(Cu) changing the copper concentration and keeping constant all the other parameters: 20, 30, 40, 50, 60, 70 and 100 g dm^{-3}
(CN) changing the cyanide concentration: 0, 20, 30, 40, 60 and 100 g dm^{-3}

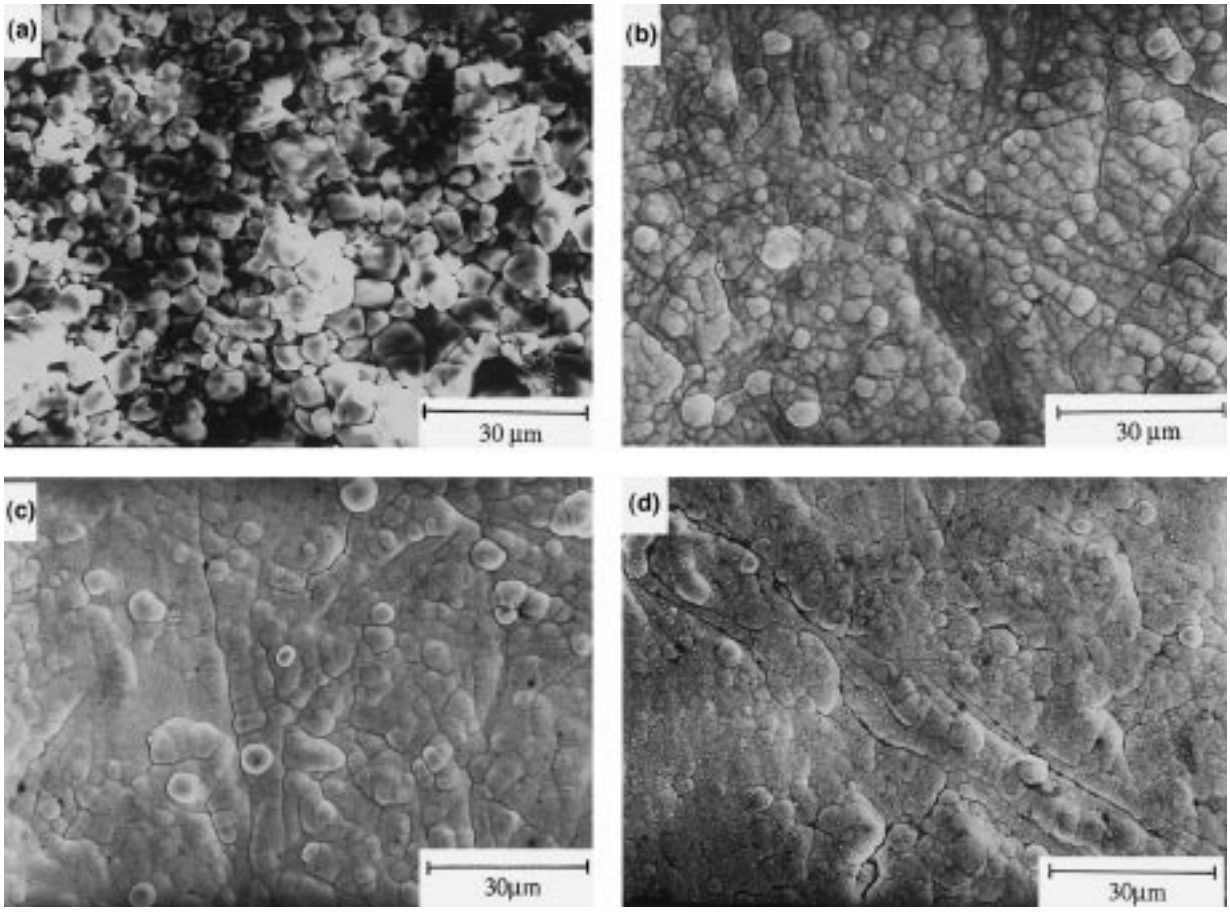

Fig. 5. Surface morphology of copper deposit at 4 μm by scanning electron microscopy. Each micrograph correspond to a different variation of standard composition: (a) time without additives (12 min), (b) time (12 min), (c) copper concentration (40 g dm^{-3}), (d) cyanide concentration (40 g dm^{-3}).

3.3. *SEM study*

The morphology of the obtained copper films depends on the synthesis conditions. Four micrographs were taken from films that, having the same thickness, were obtained under different experimental conditions (Fig. 5). The selected thickness was 4 μm, since higher values give lower differences in corrosion protection due to a pore occlusion effect. These micrographs show a granular copper plate structure. The finer granular structure correlates with a lower porosity, deduced from steady state potential measurements.

Micrograph (a) was obtained from a sample coated under standard conditions without additives and with a current density of 0.015 A cm^{-2} for 12 min. Micrograph (b) was obtained from a sample coated under standard conditions for a 12 min current flow. The morphology shown by micrograph (c) was obtained by decreasing the copper concentration to 40 g dm^{-3} and the morphology shown by micrograph (d) by increasing the cyanide concentration to 40 g dm^{-3} with respect to the standard conditions. The most irregular morphology corresponds to the film obtained from a solution without additives; in this case, the experimental area fraction obtained from the steady state potential was 1. The most homogeneous film was obtained by increasing the cyanide concentration, the area fraction being 4.7. A more irregular morphology gives a less compact film. There is little difference between micrographs (c) and (d) for area fractions of 4.4 and 4.7, respectively. The experimental area fraction of sample (b) is 4.1. The morphology of the samples correlates with the experimental corrosion potential.

4. Conclusions

The corrosion potential measurements of copper films electrodeposited on zinc diecast specimens from cyanide baths, in acid solution, have shown that the films are nonuniform and porous. Porosity, deduced from corrosion potential measurements, increases with decreasing the thickness. For a given thickness, the porosity decreases with increase in cyanide and additive concentration. The nonuniformity and porosity of the samples was demonstrated by the observed increase of the zinc concentration in a fresh industrial copper acid bath during the process.

Acknowledgement

This work was supported by the University of the Basque Country and the Ministerio de Educación y Cultura of the Spanish Government.

References

[1] G. Wranglen, 'An Introduction to Corrosion and Protection of Metals' (Chapman & Hall, London, 1985).
[2] B. L. Mckinney and C. L. Faust, *J. Electrochem. Soc.* **124** (1977) 379.
[3] L. L. Shreir, R. A. Jarman and G.T. Burstein, 'Corrosion', Vol. 2 (Butterworth–Heinemann, 3rd edn, London, 1994).
[4] J. K. Dennis and T. E. Such, 'Nickel and Chromium Plating' (Butterworths & Co, 2nd edn, London 1986).
[5] I. M. Notter and D. R. Gabe, *Corros. Rev.* **10** (1992) 217.
[6] S. C. Britton, 'Tin Versus Corrosion', ITRI publication 510.
[7] J. M. Leeds and M. Clarke, *Trans. IMF* **46** (1968) 1.
[8] R. A. Ehrhardt, Proc AES 47th Ann. Tech. **78** (1960).
[9] R. J. Morrissey and A. M. Weisberg, *Trans. IMF* **58** (1980) 97.
[10] R. Sard, Y. Okinaka and J.R. Rushton, *Plating* **58** (1971) 893.
[11] J. M. Leeds and M. Clarke, *Trans. IMF* **47** (1969) 163.
[12] K. G. Ashurst and R. W. Neale, *Trans. IMF* **45** (1965) 75.
[13] G. L. Cooksey and H. S. Campbell, *Trans. IMF* **48** (1970) 93.
[14] R. M. Angles, K.W. Caulfield and R. Kerr, *J.S.C.I.* **65** (1946) 430.
[15] R. J. Morrissey, *J. Electrochem. Soc.* **117** (1970) 742.
[16] K. B. Oldham and F. Mansfeld, *J. Appl. Electrochem.* **2** (1972) 183.
[17] E. Gileadi, 'Electrode Kinetics' (VCH, New York, 1993).
[18] L. Matuliauskienė, J. Butkevicius and A. Steponavicius, *Chemija*, **181** (1991) 115.
[19] O. Trost and B. Pihlar, *Met. Finish.* **90** (1992) 125.
[20] O. Zeimytė and A. Steponavicius, *Chemija* **2** (1992) 14.
[21] D. R. Turner and G. R. Johnson, *J. Electrochem. Soc.* **109** (1962) 798.
[22] F. Passal, *Plating* **46** (1959) 628.
[23] N. V. Parthasarady, 'Practical Electroplating Handbook' (Prentice Hall, Englewood Cliffs, NJ, 1989).